

NANO EXPRESS

Open Access



# Enhanced Ferromagnetic Interaction in Modulation-Doped GaMnN Nanorods

Yuan-Ting Lin<sup>1</sup>, Paritosh Vilas Wadekar<sup>1</sup>, Hsiang-Shun Kao<sup>1</sup>, Yu-Jung Zheng<sup>1</sup>, Quark Yung-Sung Chen<sup>1</sup>, Hui-Chun Huang<sup>2</sup>, Cheng-Maw Cheng<sup>3</sup>, New-Jin Ho<sup>2</sup> and Li-Wei Tu<sup>1,4\*</sup>

## Abstract

In this report, ferromagnetic interactions in modulation-doped GaMnN nanorods grown on Si (111) substrate by plasma-assisted molecular beam epitaxy are investigated with the prospect of achieving a room temperature ferromagnetic semiconductor. Our results indicate the thickness of GaN layer in each GaN/MnN pair, as well as Mn-doping levels, are essential for suppressing secondary phases as well as enhancing the magnetic moment. For these optimized samples, structural analysis by high-resolution X-ray diffractometry and Raman spectroscopy verifies single-crystalline modulation-doped GaMnN nanorods with Ga sites substituted by Mn atoms. Energy dispersive X-ray spectrometry shows that the average Mn concentration can be raised from 0.4 to 1.8% by increasing Mn fluxes without formation of secondary phases resulted in a notable enhancement of the saturation magnetization as well as coercive force in these nanorods.

**Keywords:** A1. Characterization, A1. Doping, A3. Molecular beam epitaxy, B1. Nanomaterials, B1. Nitrides, B2. Magnetic materials

## Background

Combining spin and charge functionalities is expected to bring a renaissance in compound semiconductors. Diluted magnetic semiconductors (DMSs) are one group of compounds where such possibilities are feasible [1]. Among potential candidates, there are group III nitrides that are widely used in commercial optoelectronic devices, such as light-emitting diodes (LEDs) and laser diodes (LDs). By enabling spin functionality, one could envision the creation of new devices or enhanced functionalities; hence, obtaining above-room-temperature ferromagnetism in nitride semiconductors is an important topic of scientific research [2]. Besides this, III nitride can be grown into nanostructures as nanocolumn LEDs and nanowire photodetector and quantum dot lasers as potential next-generation devices [3–5]. Thus, studying the possibility of incorporating spin functionality in such nanostructures has been a major goal in the scientific community [6–12]. Typically, growth of one-dimensional nanostructures such as nanowires is readily achieved by chemical vapor deposition

(CVD) [11, 13, 14], but a proper ordering of nanostructures, necessary for device fabrication, is lacking unless some extra fabrication steps are used [15]. An alternative to CVD growth is the self-assembly methodology of nanorods using plasma-assisted molecular beam epitaxy (PAMBE, Veeco) wherein no additional fabrication steps are required [16–18]. Our previous results show that it is indeed possible to incorporate Mn into GaN for creating nanostructures that exhibit room temperature ferromagnetism by incorporating a modulation-doping approach wherein a thin Mn layer is sandwiched between a thicker GaN spacer [19].

One major bottleneck for superior devices is the need for stronger magnetic signals such as saturation magnetization, remnant magnetization, and coercive force. Since the ferromagnetic properties of semiconductors depend on the amount of magnetic dopant, it is challenging to prepare thin films without the formation of any secondary phases such as ferromagnetic nanoclusters that might result in a spurious signal in magnetic measurements. Furthermore, the itinerant carriers in the host semiconductor have to couple with the localized magnetic moment and enhance the carrier-mediated ferromagnetic properties based on double exchange mechanism. The ferromagnetism of GaN-based DMSs has been reported to relate closely with the type and concentration of activated carriers

\* Correspondence: lwtu@mail.nsysu.edu.tw

<sup>1</sup>Department of Physics and Center for Nanoscience and Nanotechnology, National Sun Yat-Sen University, Kaohsiung 80424, Taiwan, Republic of China

<sup>4</sup>Department of Medical Laboratory Science and Biotechnology, Kaohsiung Medical University, Kaohsiung 80708, Taiwan, Republic of China

Full list of author information is available at the end of the article

[20, 21]. Considering all above, modulation-doping technique is adopted to obtain a high dopant concentration and carrier concentration in one or few monolayers [22]. The magnetic properties of GaN-based DMSs have been reported to be enhanced in GaMnN/GaN multilayers and GaGdN/GaN superlattice structures as compared to a single layer with normal doping method [20, 23]. In this report, we have fabricated self-aligned phase pure vertical nanorods which exhibit superior ferromagnetic properties beyond room temperature. Our investigations reveal that the amount of Mn dopant and GaN spacer thickness are crucial for the enhancement of the ferromagnetic properties as well as avoiding secondary phase formation.

## Methods

GaN nanorods were grown by plasma-assisted molecular beam epitaxy (Veeco 930) on Si (111) substrate without a buffer layer. The Si wafer was chemically cleaned before loading into the chamber and thermally cleaned after loading into the chamber as usual [19]. The growth sequence was to grow undoped GaN nanorod section first as a template, and then, modulation-doped GaMnN was grown on top of the undoped nanorod section to complete the nanorod growth. It retained the shape and vertical directions of the bottom undoped nanorod template. The modulation-doping technique utilized the metal modulation method, that is, the Mn-flux and Ga-flux modulations were achieved by controlling the open and close of the shutters of Mn and Ga while keeping the nitrogen flow uninterrupted. The metallic sources (Mn, Ga) were provided through Knudsen effusion cells and controlled by fast-action pneumatically driven shutters in front of the cells. The active nitrogen species were supplied by the radio-frequency UNI-Bulb plasma source at a fixed power of 450 W.

To study the growth of Mn modulation-doped GaN nanorods, there are two series of samples grown in this report as shown in Table 1. The substrate temperature was kept at  $T_s = 700$  °C for both series of samples. In the first series of modulation-doped GaMnN nanorods,

series I, GaN growth was interrupted 300 times through a 2-s duration of Mn flux. The thickness of GaN spacer in each pair was varied and controlled by its growth time with 5, 10, 20, and 40 s with an estimated growth rate of 0.09 nm/s. In the second series, series II, the Mn flux was raised further from  $1.7 \times 10^{-8}$  to  $2.4 \times 10^{-8}$  Torr to increase the Mn concentration of GaMnN nanorods with a total GaN/MnN growth period of 180.

The morphology and structure of nanorods were inspected by field emission scanning electron microscopy (FESEM, JEOL JSM-7000F) and high-resolution transmission electron microscopy (HRTEM, FEI Tecnai G2 F20). The concentration of Mn in GaMnN nanorods was examined by the energy dispersive X-ray spectrometry (EDS, Oxford INCA Penta FETX3) installed in the FESEM system. The phase purity of Mn modulation-doped GaN nanorods and the local structure of Mn atoms in GaN host lattice were studied by high-resolution X-ray diffractometry (HRXRD, Bede D1) and Raman spectroscopy (Jobin Yvon T64000), respectively. Furthermore, magnetic properties of GaMnN nanorods at above room temperature were carried out by using a superconducting quantum interference device (SQUID) magnetometer (Quantum Design MPMS-XL7). X-ray absorption near edge spectra (XANES) measurements of N K-edge, Ga L-edge, and Mn L-edge was performed at BL08B1 and BL20A1 beamlines of the National Synchrotron Radiation Research Center (NSRRC) in Hsinchu, Taiwan. All N K-edge, Ga L-edge, and Mn L-edge spectra were recorded at the incident beam with E-field polarization parallel to the surface of the sample at room temperature by total electron yield (TEY) mode. XANES of Mn L-edge from a MnO single crystal was taken simultaneously for the energy calibration and the comparison of different electronic valence states.

## Results and Discussion

The top and cross-sectional view of FESEM images of the modulation-doped GaMnN nanorods with 5-, 10-, 20-, and 40-s growth time of GaN spacer in GaN/MnN pair structure (labeled as samples 5s-MnNR, 10s-MnNR, 20s-MnNR, and 40s-MnNR, respectively) are shown in Fig. 1a–h, respectively. The height of these samples is 750, 850, 1200, and 1700 nm, for 5s-MnNR, 10s-MnNR, 20s-MnNR, and 40s-MnNR, respectively. The GaN spacer thickness in each pair can be estimated by the average growth rate of the nanorods, which is 0.09 nm/s. Moreover, inclinations on the top of Mn-doped GaN nanorods are observed in cross-sectional SEM image. Figure 2 shows the HRXRD spectra of modulation-doped GaMnN nanorods for the series I. The peaks at  $28.44^\circ$ ,  $34.56^\circ$ ,  $58.88^\circ$ , and  $72.90^\circ$  in  $\theta/2\theta$  scan are referred to cubic Si (111), wurtzite GaN (0002), Si (222), and GaN (0004), respectively, which also indicate that

**Table 1** Sample growth parameters and Mn concentration

	Sample	GaN/MnN pairs	Growth time per pair of GaN/MnN (s)	Mn flux ( $10^{-8}$ Torr)	EDS percentage of Mn (atomic%)
Series I	5s-MnNR	300	5/2	1.7	0.8
	10s-MnNR	300	10/2	1.7	0.7
	20s-MnNR	300	20/2	1.7	0.6
	40s-MnNR	300	40/2	1.7	0.4
Series II	S-MnNR	180	40/2	1.7	0.7
	M-MnNR	180	40/2	1.9	1.8
	L-MnNR	180	40/2	2.4	3.3

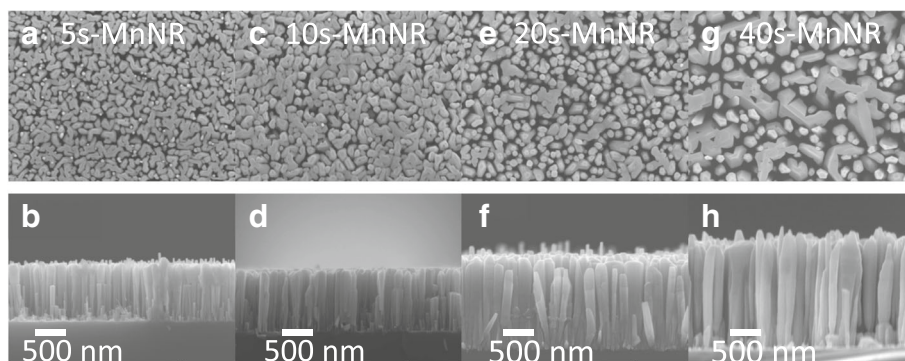


**Fig. 1** The top (a, c, e, g) and cross-sectional (b, d, f, h) view SEM images of modulation-doped GaMnN nanorods with GaN growth time in each pair as 5 s (5s-MnNR), 10 s (10s-MnNR), 20 s (20s-MnNR), and 40 s (40s-MnNR), respectively

nanorods are grown along the *c*-axis of a wurtzite structure. This wide range X-ray diffraction scan shows that there is no obvious secondary phase in sample 40s-MnNR with about 3.6 nm GaN spacer in each pair. However, an additional peak at  $46.58^\circ$ , which is referred to  $\text{Mn}_3\text{Ga}_{0.5}(200)$  [24], is observed in GaMnN nanorods while the growth time of GaN is equal to or less than 20 s. The

formation of this Mn-rich secondary phase is explained by the higher chance of more Mn ions aggregated together with the thinner GaN spacer. Mn atoms have also been proven to escape from a modulation-doped layer to the surface over a GaN layer of fewer than 11 monolayers in an MBE grown thin film at  $670^\circ\text{C}$  [25].

The microstructure of sample 40s-MnNR was studied using high-resolution TEM by measuring atomic images. Figure 3a shows a low-magnification image. The bottom region, marked as GaN, is quite clear while the top region marked as GaMnN region shows an alternation of dark and bright layers lying parallel along the nanorod diameter. To further understand the crystal structure, selected area electron diffraction (SAED) measurements were done at different positions of the nanorod. Figure 3b–d shows the SAED for the bottom, middle, and top regions of the nanorod along with the appropriate indexing. The close resemblance of the diffraction patterns indicates that integrity of the crystal structure is maintained even as Mn is incorporated. A closer inspection of the diffraction patterns in Fig. 3c, d shows some fine features such as streaking along the  $[0001]$  axis. The presence of such streaking is due to the formation of stacking faults [19]. The diffraction analysis of the sample 40s-MnNR does not show any secondary phases, collaborating with the XRD data. The Mn contents in modulation-doped GaMnN nanorods are evaluated by the EDS equipped in the SEM system as shown in Table 1. As a result, the average Mn contents of samples 5s-MnNR, 10s-MnNR, 20s-MnNR, and 40s-MnNR are read as 0.8, 0.7, 0.6, and 0.4%, respectively. The Mn concentration is reduced with the increasing growth time of GaN. This is attributed to the dilution of the average Mn concentration by the increased thickness of GaN in a GaN/MnN periodical structure.

The role of Mn atoms in GaMnN nanorods is investigated by Raman spectroscopy at room temperature with Stokes shifts as shown in Fig. 4. All samples show the

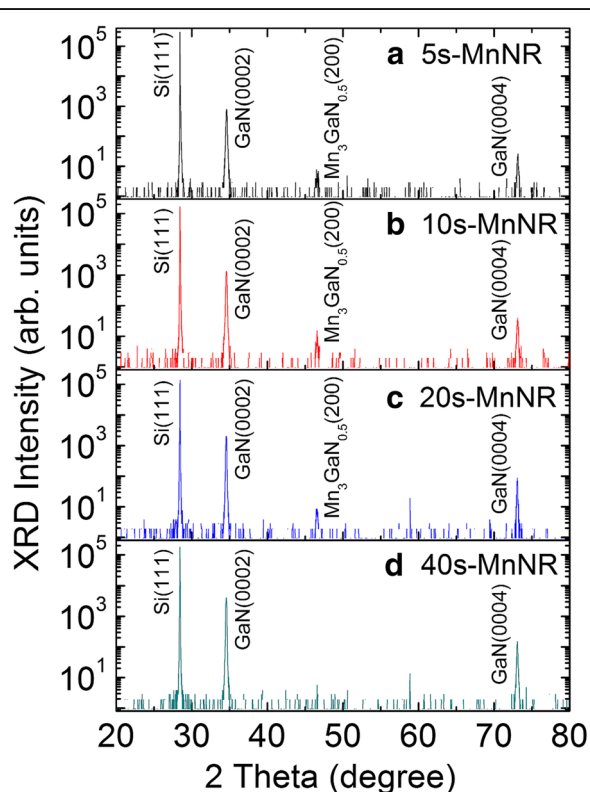
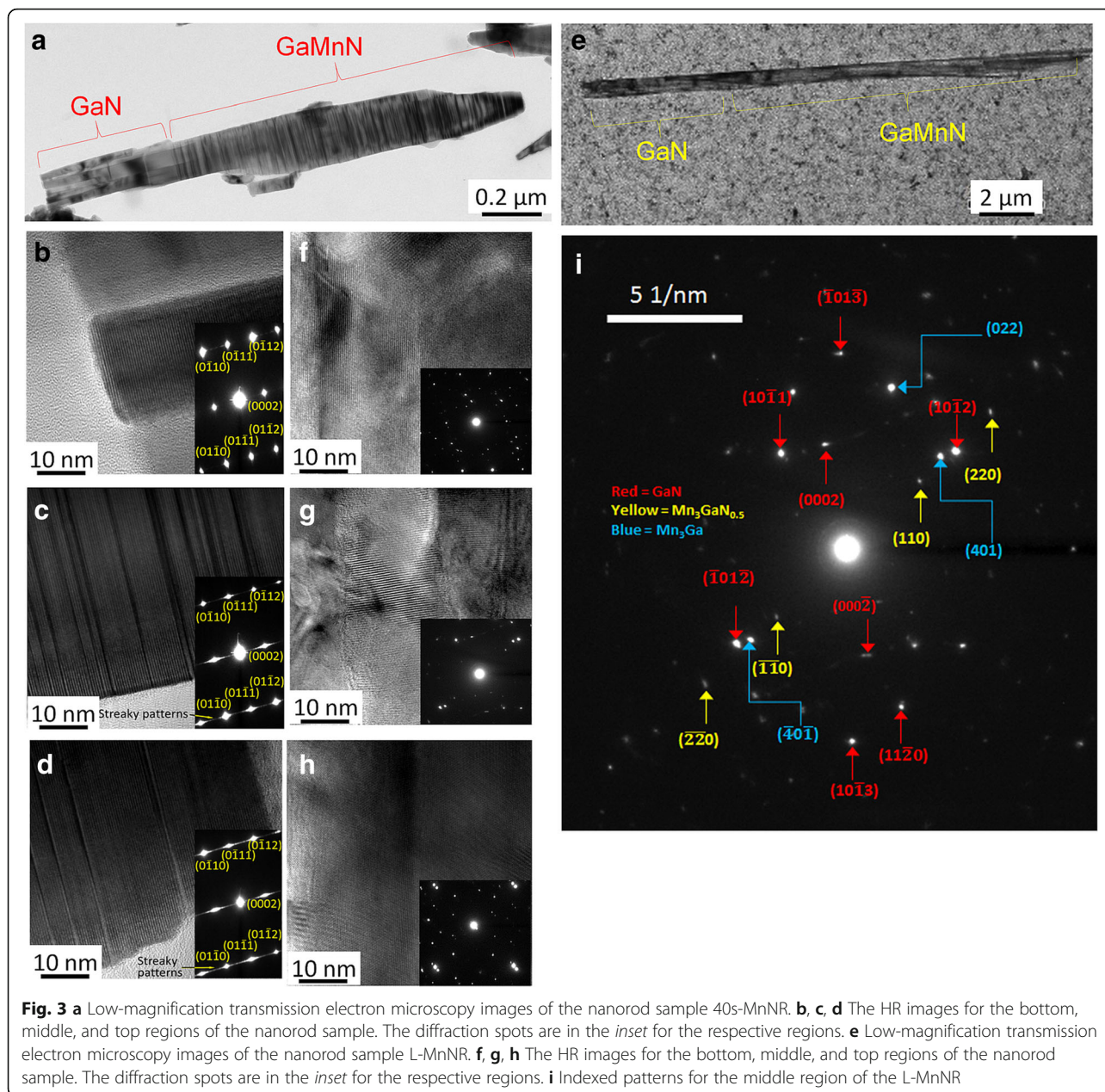


**Fig. 2** a–d HRXRD spectra of modulation-doped GaMnN nanorods with varied growth time of GaN. GaMnN nanorods with Mn-related secondary phases are observed except the sample grown with 40-s growth time of GaN spacer (40s-MnNR in d)

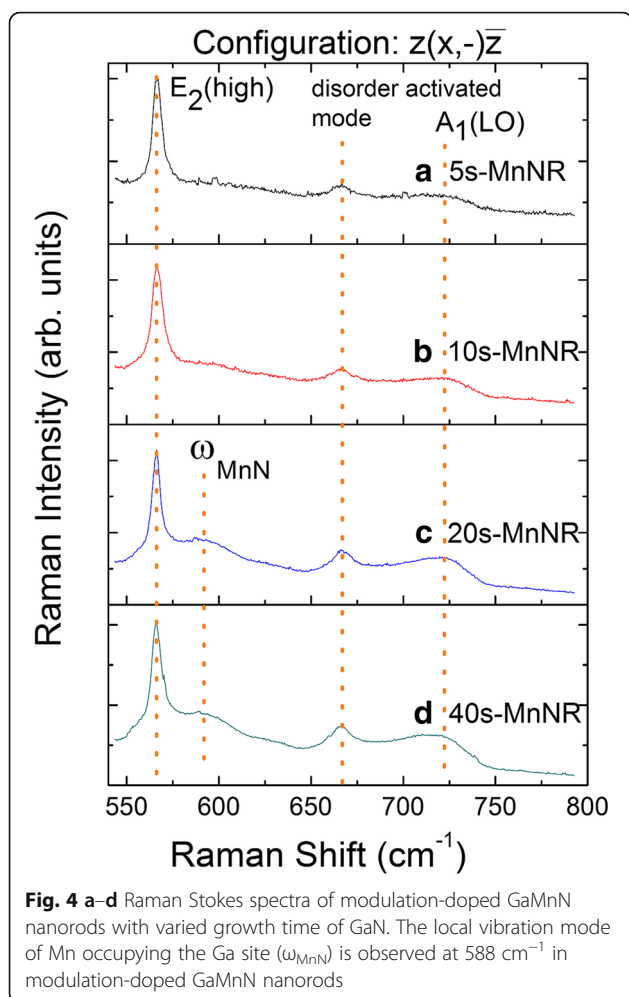




clear  $E_2(\text{high})$  mode of a wurtzite GaN at  $567\text{ cm}^{-1}$ . The presence of frequency  $\omega_{\text{MnN}}$  at  $588\text{ cm}^{-1}$  is assigned to the local vibration mode arising from Mn atoms occupying the Ga sites, which is comparable to the value of  $581\text{ cm}^{-1}$  calculated from a simple mass defect model [19, 26]. Nevertheless, the samples 5s-MnNR and 10s-MnNR, which contain higher average Mn concentration, do not reveal clear  $\omega_{\text{MnN}}$  signal. This result indicates that less Mn atoms substitute Ga atoms in GaMnN, which is consistent with the Mn-related secondary phase revealed by XRD data in GaMnN nanorods with GaN growth time equal to or less than 20 s. Furthermore, the

fairly constant signal at  $670\text{ cm}^{-1}$  is ascribed to disorder activated Raman scattering of vacancy-related defects [27]. The  $A_1(\text{LO})$  signal at  $725\text{ cm}^{-1}$  arises with the  $\omega_{\text{MnN}}$  signal. It indicates a low free carrier concentration in Mn-substituted samples [28]. This can be explained by the formation of a deep level within the GaN band-gap. Many reports on optical measurements reveal that Mn-doped GaN would create an acceptor level of 1.4–1.8 eV above the valence band [29, 30].

To further increase the Mn concentration and hopefully increase the ferromagnetic properties, a second series, series II, of samples of modulation-doped GaMnN



nanorods with varied Mn fluxes was grown. According to the results of series I, the secondary phases in modulation-doped GaMnN nanorods can be suppressed by a GaN barrier with 3.6 nm in thickness in each pair. Hence, the growth time of GaN/MnN in series II was fixed to 40/2 s, that is, the Ga shutter opens 40 s and the Mn 2 s for each period. Modulation-doped GaMnN nanorods of samples S-MnNR, M-MnNR, and L-MnNR were grown with Mn fluxes of  $1.7 \times 10^{-8}$ ,  $1.9 \times 10^{-8}$ , and  $2.4 \times 10^{-8}$  Torr, respectively. The V/III ratios were raised from 500 in series I to 1000 to further enhance the incorporation of Mn comparing samples 40s-MnNR and S-MnNR as displayed in Table 1. Figure 5 shows the EDS spectra of modulation-doped GaMnN nanorods with different Mn fluxes measured from the top of the samples. The signals of N  $K_{\alpha}$ , Ga  $L_{\alpha}$ , Si  $K_{\alpha}$ , and Mn  $K_{\alpha}$  are observed at 0.39, 1.10, 1.74, and 5.90 keV, respectively. It is noticed that the peak intensity of Mn  $K_{\alpha}$  is enhanced with the increasing Mn flux. Furthermore, the average Mn contents of S-MnNR, M-MnNR, and L-MnNR from EDS measurements are summarized in

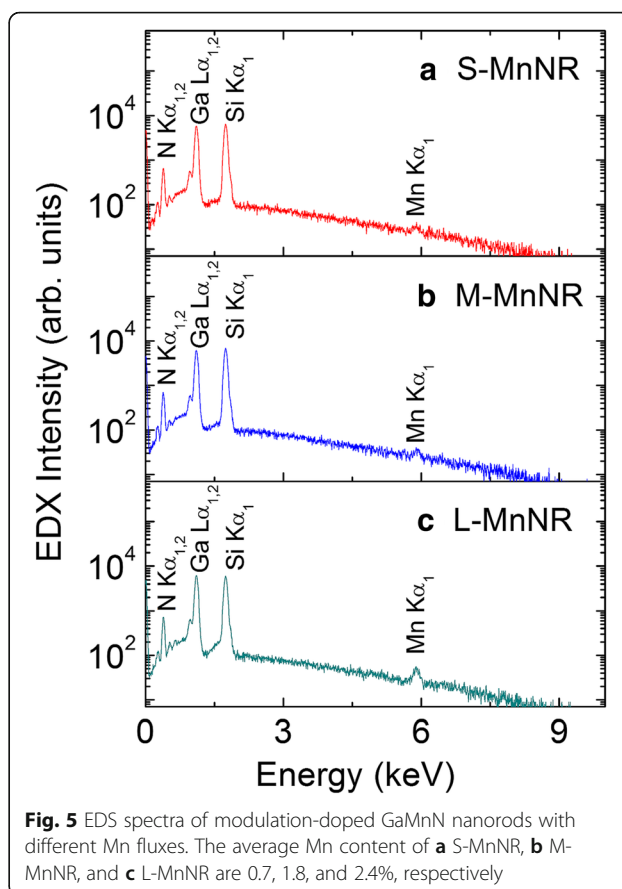
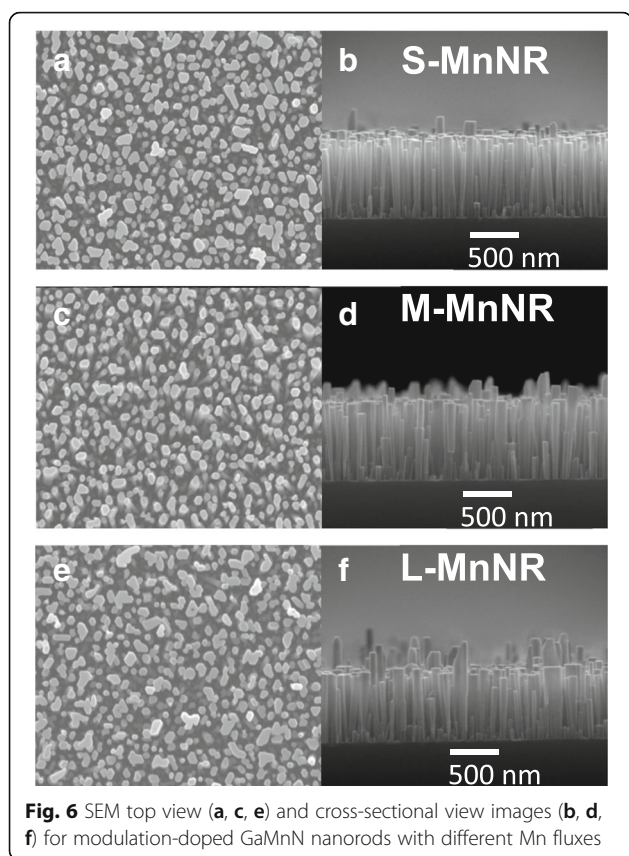
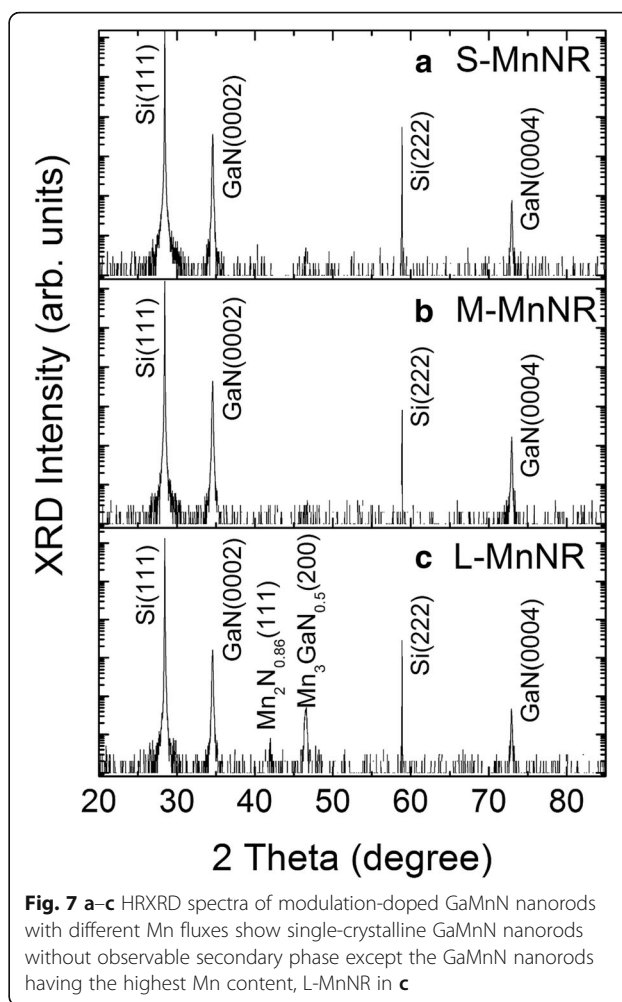


Table 1 as 0.7, 1.8, and 3.3%, respectively. Figure 6a–f shows the top and cross-sectional view of the samples S-MnNR, M-MnNR, and L-MnNR, respectively. A higher V/III ratio increases the separation of nanorod structure. With increasing Mn fluxes, the uniformity in its morphology is decreased. The GaMnN nanorods with varied Mn fluxes have similar density and about 700 nm height, as shown in cross-sectional SEM images. A little lower in height than what is expected from series I indicates possibly a little lower nitrogen plasma efficiency. All three samples show the  $\omega_{\text{MnN}}$  vibration mode in Raman spectroscopy indicating the success replacement of Ga by Mn.

The XRD  $\theta/2\theta$  spectra of modulation-doped GaMnN nanorods with different Mn fluxes are shown in Fig. 7. Like the samples in series I, single-crystalline GaMnN nanorods grown on Si (111) substrate along  $c$ -axis show main peaks at  $28.44^\circ$ ,  $34.56^\circ$ ,  $58.88^\circ$ , and  $72.90^\circ$  referred to cubic Si (111), wurtzite GaN (0002), Si (222), and GaN (0004) diffractions, respectively. However, the secondary phases of  $\text{Mn}_2\text{N}_{0.86}$  (111) and  $\text{Mn}_3\text{Ga}_{0.5}$  (200) are observed at  $42.00^\circ$  and  $46.58^\circ$  in heavily Mn-doped GaN nanorod, sample L-MnNR [31, 32], which indicates that the average 3.3% Mn concentration has exceeded the solubility of Mn in these GaN nanorods to



form  $\text{Ga}_{1-x}\text{Mn}_x\text{N}$  with Mn substituting the Ga under the growth conditions. In comparison, MBE grown GaMnN thin films with Mn concentration higher than 6% and up to 8.2% have been reported [33, 34]. Lower solubility of Mn in GaN nanorods can be attributed to the higher growth temperature [35, 36]. Mn-related precipitates are more easily formed in MBE growth with increased temperature [37]. The other possibility is the higher than average value near the MnN layers in these samples which are then averaged out by the GaN layers. We have used HRTEM to identify if such secondary phases can be observed. Figure 3e shows the low-magnification imaging for the multiphase L-MnNR sample while Fig. 3f–h shows the atomic imaging for the different regions. Comparing the multiphase sample to the single-phase sample 40s-MnNR in Fig. 3a–d, the layering in single-phase sample is absent in the multiphase one. The SAED patterns from various regions of the multiphase sample are also shown in the insets which show many diffraction spots. It is difficult to find one periodic ordering that will successfully index all the spots. We selected the diffraction pattern from the middle region which is less complex as compared to the other two and tried to identify the various phases present as in Fig. 3i. By measuring the distance from the



center spot to the other spots, we calculated the reciprocal lattice vectors and compared them to known values from literature for GaN, GaMn, and Ga-Mn-N compounds. Some of the bright spots can be indexed to wurtzite GaN lying along the *m*-zone ( $10\bar{1}l$ ) and *c*-zone ( $000l$ ) (labeled in red). The other strong set of spots was indexed to orthorhombic  $\text{Mn}_3\text{Ga}$  (labeled in blue), while the weak spots were indexed to  $\text{Mn}_3\text{Ga}_{0.5}$  (labeled in yellow). So while it is difficult to image a nanocluster in the imaging mode, SAED measurements can be useful for the analysis.

We have studied the electronic properties of the single-phase samples by XANES. The various spectra are plotted in Fig. 8a–c for N K-edge, Ga L-edge, and Mn L-edge, respectively. As seen, no obvious differences in the Ga or the N signal are seen for the Mn-doped samples as compared to the reference undoped GaN nanorod sample implying that that local electronic structure is the same. The valence state of Mn is +2 as judged by the same peak shapes in the Mn-doped samples as compared to the reference sample which is MnO single



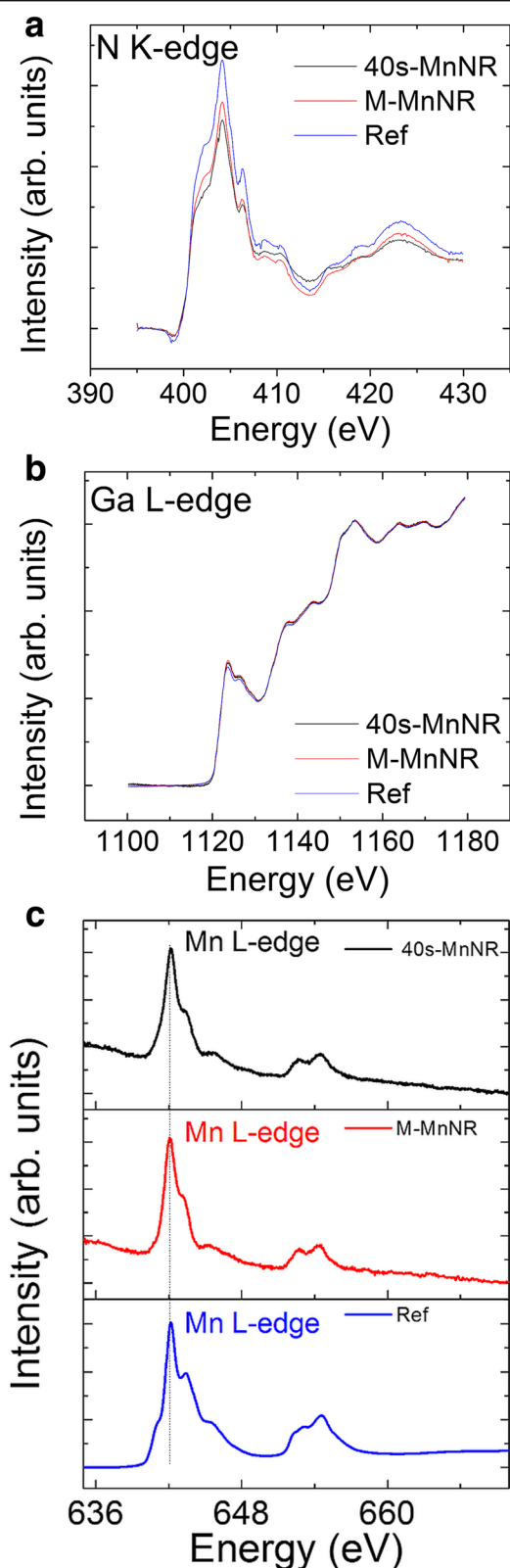


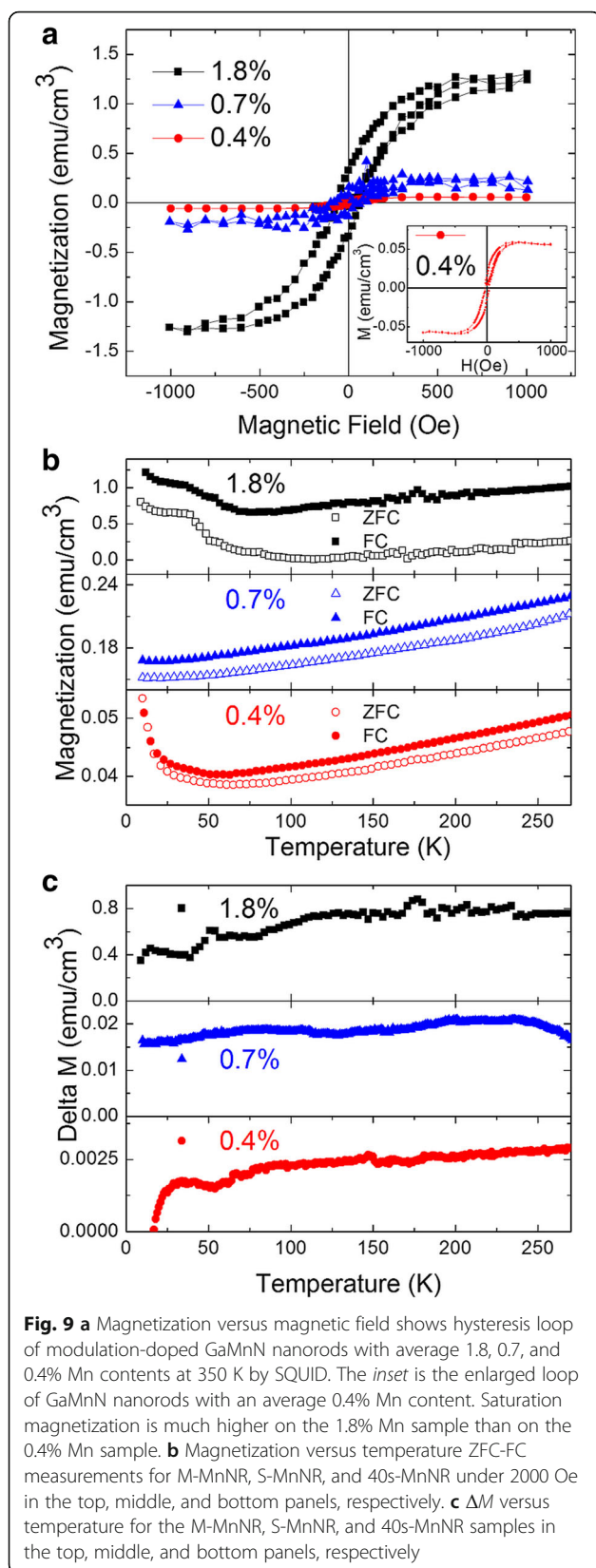
**Fig. 8** XANES spectra for N K-edge, Ga L-edge, and Mn L-edge are plotted in **a**, **b**, and **c**, respectively. Reference sample in **a** and **b** is undoped GaN nanorod sample and in **c** MnO single crystal

crystal and with other reported results for Mn-doped GaN [38–40].

Investigations of the magnetic properties of modulation-doped GaMnN nanorods were carried out by magnetization versus magnetic field ( $M$  vs.  $H$ ) measurements at room temperature. However, the  $\text{Mn}_2\text{N}_{0.86}$  has been demonstrated as a weak ferromagnetic material at room temperature besides dominant antiferromagnetism [32, 41]. To avoid the possible ferromagnetism contributed from secondary phases, the modulation-doped GaMnN nanorods without secondary phases were chosen for subsequent magnetic properties studies. In Fig. 9a, the magnetization versus magnetic field curves at 350 K for samples 40s-MnNR, S-MnNR and M-MnNR are plotted. A linear background from the raw data was subtracted to extract the signal from the nanorods. The inset  $M$  vs.  $H$  shows the enlarged hysteresis effect of GaMnN nanorods with an average 0.4% Mn content. An above-room-temperature ferromagnetism is evidenced by the clear hysteresis loops in all three samples. By adjusting the Mn-doping concentration and the GaN spacers, the saturated magnetization of nanorods increases by almost 25 times indicating a positive correlation with the total spin moment of the material. We also did zero-field-cooled and field-cooled (ZFC-FC) measurements for the single-phase samples by sweeping the temperature and measuring magnetization. These measurements were done at a magnetic field of 2000 Oe. The top, middle, and bottom panels of Fig. 9b show the data for samples M-MnNR, S-MnNR, and 40s-MnNR, respectively. The splitting between the magnetization starts near room temperature and is the strongest for M-MnNR. As the sample is cooled down, magnetization starts to decrease slightly, and at very low temperatures, there is an upturn. This could be due to some paramagnetic signal. An important point to note is the absence of any blocking temperature behavior in the ZFC-FC measurements, implying that samples are free from clusters or secondary phases, corroborating with the XRD and TEM data. The difference in the magnetization ( $\Delta M = M_{\text{FC}} - M_{\text{ZFC}}$ ) is also plotted in Fig. 9c. One can clearly see strong magnetization near room temperature suggesting that the ferromagnetic transition is at room temperature with the strongest signal in M-MnNR.

## Conclusions

The MBE growth and characteristics of modulation-doped GaMnN nanorods have been systematically investigated. The thickness of GaN in each pair of GaN/MnN was varied by the growth time of GaN. A thick GaN spacer with the 40-s growth time between Mn modulation-doped layers reduces the possibility of excess Mn atom aggregation and suppresses the formation of secondary phases effectively. Modulation-doped GaMnN nanorods



with varied Mn fluxes were also investigated to achieve single-crystalline GaMnN nanorods with higher Mn content. Samples grown under Mn fluxes of  $1.7 \times 10^{-8}$  and  $1.9 \times 10^{-8}$  Torr have a Mn concentration of 0.7 and 1.8%, respectively, measured by EDS, and no secondary phases were observed by XRD. Raman scattering indicates the substitution of Ga by Mn atoms. Zero-field-cooled and field-cooled measurements reveal no clusters or secondary phases. Hysteresis loops in magnetization versus magnetic field measurements of GaMnN nanorods show above-room-temperature ferromagnetism, and the saturation magnetizations are enhanced with increasing Mn content which shows a positive correlation. This opens a possible route to applications in nanostructural spintronics.

#### Abbreviations

CVD: Chemical vapor deposition; DMSs: Diluted magnetic semiconductors; EDS: Energy dispersive X-ray spectrometry; FESEM: Field emission scanning electron microscopy; HRTEM: High-resolution transmission electron microscopy; HRXRD: High-resolution X-ray diffractometry; LDs: Laser diodes; LEDs: Light-emitting diodes; M vs. H: Magnetization versus magnetic field; NSRRC: National Synchrotron Radiation Research Center; PAMBE: Plasma-assisted molecular beam epitaxy; SQUID: Superconducting quantum interference device; TEY: Total electron yield; XANES: X-ray absorption near edge spectra; ZFC-FC: Zero-field-cooled and field-cooled

#### Acknowledgements

We would like to acknowledge and thank Dr. H. D. Yang for providing access to the SQUID facilities for magnetometry studies.

#### Funding

This work is supported by the Ministry of Science and Technology (MOST) of Taiwan, Republic of China, under grant numbers 99-2119-M-110-005-MY3, 102-2112-M-110-004-MY3, and 105-2112-M-110-005. We would also like to acknowledge the additional funding support from Ministry of Education (MOE) of Taiwan for the 5Y50B program.

#### Authors' Contributions

YTL, YJZ, and HSK grew the samples and did the XRD, Raman, and SEM measurements. HC and NJ helped with the TEM measurements. CMC did the XANES measurements. YTL and PW wrote and analyzed the data and wrote the manuscript. LWT revised the manuscript. LWT and QYC supervised the work and offered suggestions. All authors read and approved the final manuscript.

#### Competing Interests

The authors declare that they have no competing interests.

#### Publisher's Note

Springer Nature remains neutral with regard to jurisdictional claims in published maps and institutional affiliations.

#### Author details

<sup>1</sup>Department of Physics and Center for Nanoscience and Nanotechnology, National Sun Yat-Sen University, Kaohsiung 80424, Taiwan, Republic of China.

<sup>2</sup>Department of Materials and Optoelectronic Science and Center for Nanoscience and Nanotechnology, National Sun Yat-Sen University, Kaohsiung 80424, Taiwan, Republic of China. <sup>3</sup>National Synchrotron Radiation Research Center, Hsinchu 30076, Taiwan, Republic of China. <sup>4</sup>Department of Medical Laboratory Science and Biotechnology, Kaohsiung Medical University, Kaohsiung 80708, Taiwan, Republic of China.



Received: 15 December 2016 Accepted: 7 April 2017

Published online: 20 April 2017

## References

- Ohno H (1998) Making nonmagnetic semiconductors ferromagnetic. *Science* 281:951–956
- Liu C, Yun F, Morkoç H (2005) Ferromagnetism of ZnO and GaN: a review. *J Mater Sci Mater Electron* 16:555–597
- Sekiguchi H, Kishino K, Kikuchi A (2010) Emission color control from blue to red with nanocolumn diameter of InGaN/GaN nanocolumn arrays grown on same substrate. *Appl Phys Lett* 96:96–99
- Bugallo ADL, Tchernycheva M, Jacopin G et al (2010) Visible-blind photodetector based on p-i-n junction GaN nanowire ensembles. *Nanotechnology* 21:315201
- Wang Q, Wang T, Bai J et al (2008) Growth and optical investigation of self-assembled InGaN quantum dots on a GaN surface using a high temperature AlN buffer. *J Appl Phys* 103:123522
- Radovanovic PV, Barrelet CJ, Gradec S, Lieber CM (2005) General synthesis of manganese-doped II–VI and III–V semiconductor nanowires. *Nano* 5:1407–1411
- Wang Q, Sun Q, Jena P (2005) Ferromagnetism in Mn-doped GaN nanowires. *Phys Rev Lett* 95:167202
- Seong HK, Kim JY, Kim JJ et al (2007) Room-temperature ferromagnetism in Cu doped GaN nanowires. *Nano Lett* 7:3366–3371
- Stamplecoskie KG, Ju L, Farvid SS, Radovanovic PV (2008) General control of transition-metal-doped GaN nanowire growth: toward understanding the mechanism of dopant incorporation. *Nano Lett* 8:2674–2681
- Li Y, Cao C, Chen Z (2010) Ferromagnetic Fe-doped GaN nanowires grown by chemical vapor deposition. *J Phys Chem C* 114:21029–21034
- Farvid SS, Hegde M, Hosein ID, Radovanovic PV (2011) Electronic structure and magnetism of Mn dopants in GaN nanowires: ensemble vs single nanowire measurements. *Appl Phys Lett* 99:10–13
- Hegde M, Farvid SS, Hosein ID, Radovanovic PV (2011) Tuning manganese dopant spin interactions in single GaN nanowires at room temperature. *ACS Nano* 5:6365–6373
- Han DS, Park J, Rhie KW et al (2005) Ferromagnetic Mn-doped GaN nanowires. *Appl Phys Lett* 86:1–3
- Choi H-J, Seong H-K, Chang J et al (2005) Single-crystalline diluted magnetic semiconductor GaN:Mn nanowires. *Adv Mater* 17:1351–1356
- Deb P, Kim H, Rawat V et al (2005) Faceted and vertically aligned GaN nanorod arrays fabricated without catalysts or lithography. *Nano Lett* 5:1847–1851
- Seo HW, Chen QY, Tu LW et al (2005) Catalytic nanocapillary condensation and epitaxial GaN nanorod growth. *Phys Rev B* 71:1–5
- Tu LW, Hsiao CL, Chi TW et al (2003) Self-assembled vertical GaN nanorods grown by molecular-beam epitaxy. *Appl Phys Lett* 82:1601–1603
- Hsiao CL, Tu LW, Chi TW et al (2006) Buffer controlled GaN nanorods growth on Si(111) substrates by plasma-assisted molecular beam epitaxy. *J Vac Sci Technol B Microelectron Nanom Struct* 24:845
- Lin YT, Wadekar PV, Kao HS et al (2014) Above room-temperature ferromagnetism of Mn delta-doped GaN nanorods. *Appl Phys Lett* 104:62414
- Liu C, Gao X, Tao D et al (2015) Structural, Raman scattering and magnetic characteristics of Er<sup>3+</sup>-implanted GaN thin films. *J Alloys Compd* 618:533–536
- Ji C, Yang X, Jiang X et al (2014) Structure dependence of magnetic properties for annealed GaMnN films grown by MOCVD. *Chinese Phys Lett* 31:67501
- Schubert EF, Kuo JM, Kopf RF et al (1990) Beryllium  $\delta$  doping of GaAs grown by molecular beam epitaxy. *J Appl Phys* 67:1969
- Zhou Y, Choi S, Kimura S et al (2010) Structural and magnetic properties of GaGdN/GaN superlattice structures. *Thin Solid Films* 518:5659–5661
- Kim KH, Lee KJ, Park JB et al (2003) GaMnN thin films grown on sapphire and GaAs substrates using single GaN precursor via molecular beam epitaxy. *J Korean Phys Soc* 42:S399–S402
- Shi M, Chinchore A, Wang K et al (2012) Formation of manganese  $\delta$ -doped atomic layer in wurtzite GaN. *J Appl Phys* 112:53517
- Harima H (2004) Raman studies on spintronics materials based on wide bandgap semiconductors. *J Phys Condens Matter* 16:S5653
- Limmer W, Ritter W, Sauer R et al (1998) Raman scattering in ion-implanted GaN. *Appl Phys Lett* 72:2589
- Gebicki W, Strzeszewski J, Kamler G et al (2000) Raman scattering study of Ga<sub>1-x</sub>Mn<sub>x</sub>N crystals. *Appl Phys Lett* 76:3870
- Graf T, Gjukic M, Brandt MS et al (2002) The Mn<sup>3+/2+</sup> acceptor level in group III nitrides. *Appl Phys Lett* 81:5159–5161
- Korotkov RY, Gregie JM, Wessels BW (2002) Optical properties of the deep Mn acceptor in GaN:Mn. *Appl Phys Lett* 80:1731–1733
- Liu Y, Xu L, Li X et al (2010) Growth and magnetic property of  $\zeta$ -phase Mn<sub>2</sub>N<sub>1+x</sub> thin films by plasma-assisted molecular beam epitaxy. *J Appl Phys* 107:103914
- Sun ZH, Song XY, Yin FX et al (2009) Giant negative thermal expansion in ultrafine-grained Mn<sub>3</sub>(Cu<sub>1-x</sub>Ge<sub>x</sub>)N(x = 0.5) bulk. *J Phys D Appl Phys* 42:122004
- Sonoda S, Tanaka I, Ikeno H et al (2006) Coexistence of Mn<sup>2+</sup> and Mn<sup>3+</sup> in ferromagnetic GaMnN. *J Phys Condens Matter* 18:4615–4621
- Hu B, Man BY, Yang C et al (2011) The important role of Mn<sup>3+</sup> in the room-temperature ferromagnetism of Mn-doped GaN films. *Appl Surf Sci* 258:525–529
- Ristić J, Calleja E, Fernández-Garrido S et al (2008) On the mechanisms of spontaneous growth of III-nitride nanocolumns by plasma-assisted molecular beam epitaxy. *J Cryst Growth* 310:4035–4045
- Kikuchi A, Kawai M, Tada M, Kishino K (2004) InGaN/GaN multiple quantum disk nanocolumn light-emitting diodes grown on (111) Si substrate. *Jpn J Appl Phys* 43:L1524
- Kondo T, Kuwabara S, Owa H, Munekata H (2002) Molecular beam epitaxy of (Ga, Mn) N. *J Cryst Growth* 239:1353–1357
- Soo YL, Kioseoglou G, Kim S et al (2001) Local structure and chemical valency of Mn impurities in wide-band-gap III–V magnetic alloy semiconductors Ga<sub>1-x</sub>Mn<sub>x</sub>N. *Appl Phys Lett* 79:3926–3928
- Bacewicz R, Filipowicz J, Podsiadło S et al (2003) Probing local order in (Ga, Mn)N alloys by X-ray absorption spectroscopy. *J Phys Chem Solids* 64:1469–1472
- Titov A, Biquard X, Halley D et al (2005) X-ray absorption near-edge structure and valence state of Mn in (Ga, Mn)N. *Phys Rev B* 72:1–7
- Feng WJ, Sun NK, Du J et al (2008) Structural evolution and magnetic properties of Mn–N compounds. *Solid State Commun* 148:199–202

**Submit your manuscript to a SpringerOpen<sup>®</sup> journal and benefit from:**

- Convenient online submission
- Rigorous peer review
- Immediate publication on acceptance
- Open access: articles freely available online
- High visibility within the field
- Retaining the copyright to your article

Submit your next manuscript at ► [springeropen.com](http://springeropen.com)